scientific reports

Check for updates

OPEN

Semi-automated evaluation of trabecular meshwork and schlemm canal imaged with OCT in children with normal eyes vs. primary congenital glaucoma

Bo Wang[1,4]✉, Alden P. Gregston[2,4], Rizul Naithani[2], Samuel Alvarez[3], Rohini R. Sigireddi[2] & Sharon F. Freedman[2]

Maldevelopment of Schlemm canal (SC) and trabecular meshwork (TM) is proposed in the pathogenesis of primary congenital glaucoma (PCG). This study aims to evaluate a semi-automated segmentation algorithm of SC and TM in pediatric patients scanned using overhead-mounted optical coherence tomography (OCT). Twenty-four children (33 eyes: 17 PCG, 16 normal), with mean age 1.3 ± 1.08 years, had anterior segment OCT imaging. Manual segmentation of SC and TM on individual B-scans represented the gold standard and was compared to semi-automated segmentation of the same structures. Intraclass correlation (ICC) compared the manual and semi-automated algorithm for several parameters: SC area (0.940), circularity (0.742), and aspect ratio (0.861); and TM thickness (0.807). Comparing eyes with PCG vs. normal, we found: (1) decreased SC area (4084 ± 4553μm^2 vs. 7362 ± 3961μm^2, $p = 0.008$), (2) increased SC circularity (0.46 ± 0.15 vs. 0.36 ± 0.14, $p = 0.011$, 3) increased TM thickness (152 ± 43 μm vs. 110 ± 27 μm, $p < 0.001$) and 4) decreased SC aspect ratio (5.35 ± 2.51 vs. 7.06 ± 2.48, $p = 0.012$) in eyes with PCG. Semi-automated segmentation permits assessment of differences in SC and TM morphology in normal vs. PCG eyes. Further work is necessary to understand how SC and TM differ in these patients as well as other forms of childhood glaucoma.

Primary congenital glaucoma (PCG) is a rare disease associated with significant morbidity for affected patients and their families[1,2]. Maldevelopment of the trabecular meshwork (TM) and Schlemm canal (SC) specifically are thought to play a critical role in the pathogenesis of PCG[3,4]. Many of the first line surgical treatments involve attempting to improve aqueous outflow by addressing these pathological structures[4].

Anterior segment optical coherence tomography (AS-OCT), a non-invasive imaging methodology, can demonstrate features of the angle in adults and children, and could be valuable in the evaluation of adult and childhood glaucoma[5]. SC area has been shown to be smaller in adults with primary open angle glaucoma[6,7]. SC has been shown to be more commonly collapsed in eyes with PCG[8]. The purpose of this study is to test a semi-automated method for segmentation and quantification of the TM and SC using anterior segment optical coherence tomography (AS-OCT). An additional goal of this endeavor is to better characterize quantitative differences observed in angle structures between children's eyes with PCG and normal eyes.

Materials and methods

This study, approved by the Institutional Review Board of Duke University Hospital, conformed to the requirements of the US Health Insurance Portability and Accountability Act of 1996 and all tenets of the Declaration of Helsinki. Written informed consent was obtained from the legal guardian.

Participants

Consecutive children undergoing clinically-indicated anesthesia (such as prior to strabismus or chalazion surgery for children with healthy eyes, prior to planned exams under anesthesia, and prior to glaucoma surgery

[1]Department of Ophthalmology, Wilmer Eye Institute, Johns Hopkins Medicine, Baltimore, MD, USA. [2]Department of Ophthalmology, Duke University Medical Center, Durham, NC, US. [3]Department of Neurology, State University of New York Downstate, Brooklyn, NY, USA. [4]Bo Wang MD, PhD and Alden P. Gregston MD contributed equally to this work. ✉email: wang.bo@jhmi.edu

for children with PCG) were recruited into this prospective study. All eyes were imaged using the Spectralis SD-OCT system with FLEX module (software V.5.1.3.0, Heidelberg-Engineering, Dossenheim, Germany, FLEX-OCT) as a part of an ongoing prospective study using the investigational overhead-mounted OCT device. We selected eyes without any prior intraocular surgery in children younger than 6 years of age with either a diagnosis of primary congenital glaucoma or no intraocular pathology (normal). The contralateral eye of child with non-traumatic unilateral cataract was considered normal. The contralateral eye of a child with unilateral primary congenital glaucoma was not considered to be normal. Exclusion criteria included any eyes with a history previous intraocular surgery, trauma, or known anterior segment dysgenesis.

Imaging

FLEX-OCT was performed by a trained ophthalmic photographer or pediatric ophthalmologist in all patients. The imaging protocol included obtaining a 20° by 10° volume (7.5 mm x 3.75 mm x 1.9 mm) through the nasal and temporal angle of each eye (comprising about 10° of the angle in each scan). Total imaging time was limited to 15 min total for both eyes. An attempt was made to image both eyes of each enrolled child.

Analysis

A masked observer selected two to three representative slices from each included eye for a total of 82 representative AS-OCT slices. All slices selected were at least 50 µm apart. Two masked physicians (manual segmentation 1 and manual segmentation 2) and a semi-automated algorithm (using ImageJ and MATLAB) independently segmented the TM and SC in each image slice.

The semi-automated algorithm requires the user to select the approximate region where SC and TM are located. Once seeding is completed, median filter and local contrast enhancement are performed to improve visibility of SC and local thresholding is performed using Otsu method in ImageJ. The image is then masked based on the seeding to acquire the final segmentation (Fig. 1).

The following parameters were analyzed: SC area, SC circularity, SC aspect ratio and TM thickness. SC area, circularity and aspect ratio were computed using the ImageJ particle analysis function[9]. Aspect ratio is defined as the ratio between the major and minor axis of the ellipsoid that fits the object. Circularity is defined as the ratio between area and the perimeter squared (the ratio is multiplied by 4π so that a perfect circle would have a circularity of 1). TM thickness was calculated using local thickness in ImageJ, which finds the average of the largest circles that fit within the desired structure at a given point[9,10]. For each measured parameter, interclass correlation (ICC) was compared between the average of the two graders versus the semi-automated algorithm. For the purpose of this study, ICC ≥ 0.9 was considered excellent, 0.75 ≤ ICC < 0.90 was considered good correlation, 0.5 ≤ ICC < 0.75 moderate and ≤ 0.5 poor correlation. Parameters measured were compared between PCG and normal eyes using a linear mixed effect model to account for the use of both eyes in some

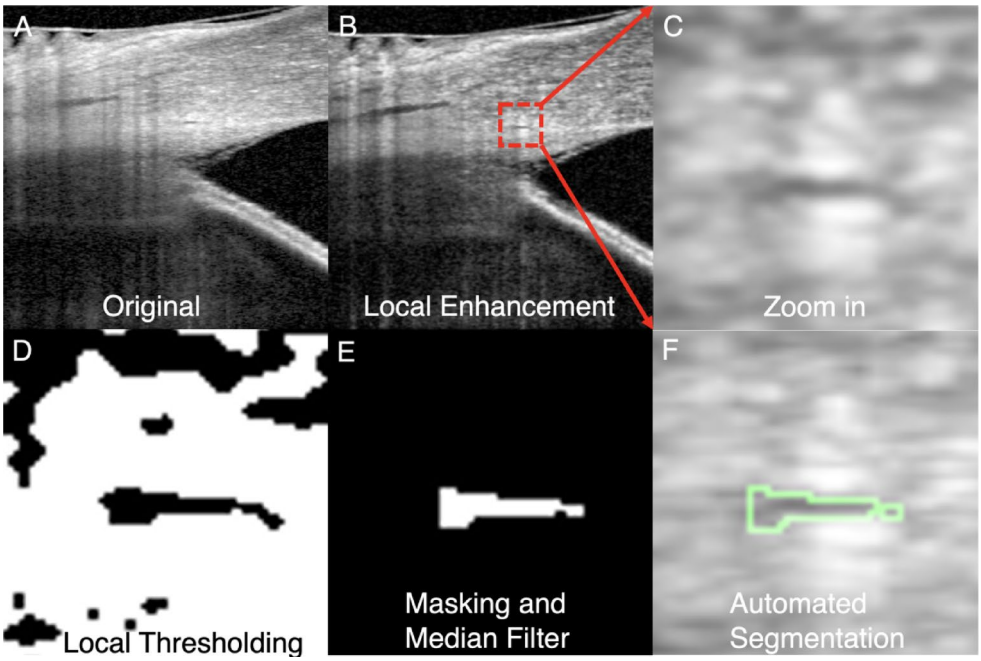

Fig. 1. Semi-automated segmentation process for Schlemm canal (SC) in a child with primary congenital glaucoma. (**A**) Original OCT slice demonstrating location of SC and size of the exterior mask; note the smaller Schlemm canal and prominent trabecular meshwork in this image. (**B**) Local contrast enhancement is performed to highlight local structure of the SC. (**C**) Zoomed in image demonstrates SC detail. (**D**) Local thresholding is performed to isolate small hypo-reflective areas within the image. (**E**) Exterior masking is applied along with median filter to smooth out the edges. (**F**) Results of the semi-automated segmentation (green) is overlain.

	Normal	PCG	*P*-value
Participants	12 (16 eyes)	12 (17 eyes)	
Age (years)	1.9 ± 1.0	0.8 ± 0.9	< 0.001
IOP (mmHg)	15.1 ± 4.3	27.1 ± 6.9	< 0.001
Number of glaucoma medications	0.0 ± 0.0	2.3 ± 0.8	< 0.001

Table 1. Demographic information for the normal and primary congenital glaucoma eyes.

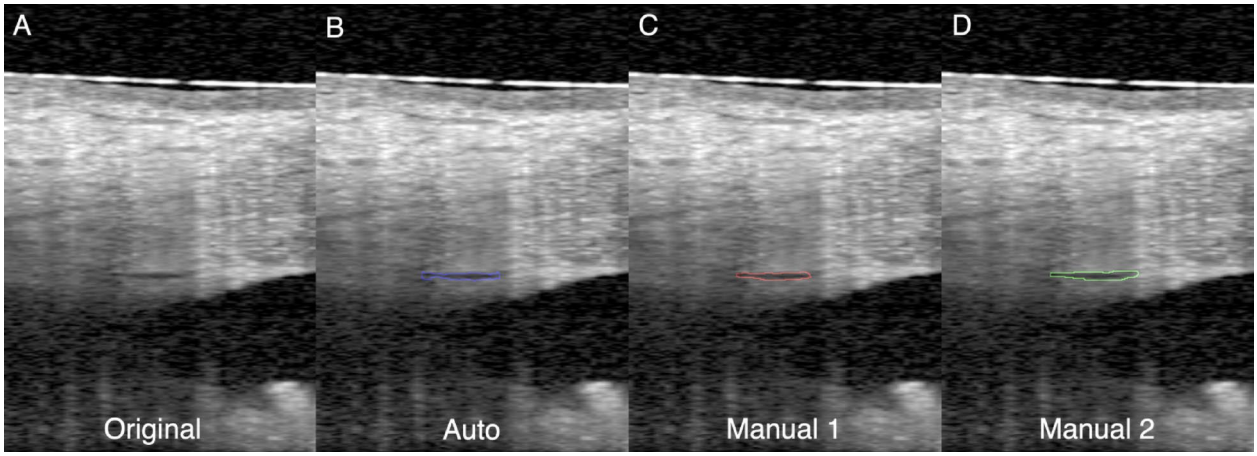

Fig. 2. Example of segmentation of Schlemm canal in a normal eye showing the (**A**) original image, (**B**) semi-automated segmentation (overlay in blue), (**C**) manual segmentation 1 and (**D**) manual segmentation 2.

patients and multiple images per eye. In addition, a linear mixed effect model was used to evaluate the how the parameters were related to each other, as well as intraocular pressure (IOP), while accounting for disease status.

Results

Thirty-three eyes (24 children) were included, including 16 normal eyes (12 children) and 17 eyes with PCG (12 children). Four normal eyes were excluded due to insufficient image quality. Two normal eyes were contralateral eyes of unilateral cataract patients. The mean age of included children at imaging was 1.35 ± 1.15 years. There was a significant difference in the age, IOP and number of glaucoma medication between the normal and PCG eyes (Table 1).

Using the average of the two manual segmentation readings for each parameter as gold standard, intraclass correlation (ICC) were as follows: 0.940 for SC area, 0.742 for SC circularity, 0.861 for SC aspect ratio, and 0.807 for TM thickness. Individual comparisons for ICC between different groups are shown in Supplemental Table 1, which demonstrate that the mean difference between semi-automated vs. manual segmentation is similar to the difference between the two different manual segmentations. Examples of the semi-automated and manual segmentation are shown in Figs. 2 and 3, showing more variability in the segmentation of the TM than in other measured parameters (Fig. 3).

Using the semi-automated segmentation, average SC area for normal vs. PCG eyes, respectively, was 7362 ± 3961μm^2 vs. 4084 ± 4553μm^2, $p = 0.008$. Similarly, semi-automated segmentation found mean SC aspect ratio for normal vs. PCG eyes, respectively, was 7.7 ± 2.3 vs. 5.35 ± 2.51, $p = 0.012$; mean SC circularity for normal vs. PCG eyes, respectively, was 0.36 ± 0.14 vs. 0.46 ± 0.15, respectively, $p = 0.011$; and mean TM thickness for normal vs. PCG eyes, respectively, was 110 ± 27 μm vs. 152 ± 43 μm, $p < 0.001$. The data is summarized in Fig. 4. This trend remained the same for SC area and SC circularity with both manual segmentations (Supplemental Figs. 1 and 2). However, manual segmentation 2 did not show a statistically significant difference in TM thickness between PCG and normal eyes. Neither manual segmentations identified SC aspect ratio as different between PCG and normal eyes.

Accounting for the effect of diagnosis, there was a negative association between SC area and TM thickness (Fig. 5A). Every micron increase in TM thickness was associated with a 41.2 ± 13.4μm^2 ($p = 0.003$) decrease in SC area. There was no effect of IOP on either TM thickness ($p = 0.276$) or SC area ($p = 0.389$) after accounting for the effect of diagnosis (Fig. 5B and C) on the relationship.

The data did not show a statistically significant difference in SC area ($p = 0.924$), aspect ratio (0.394), circularity ($p = 0.198$), or TM thickness ($p = 0.489$) comparing the nasal and temporal quadrants, for either PCG or normal eyes.

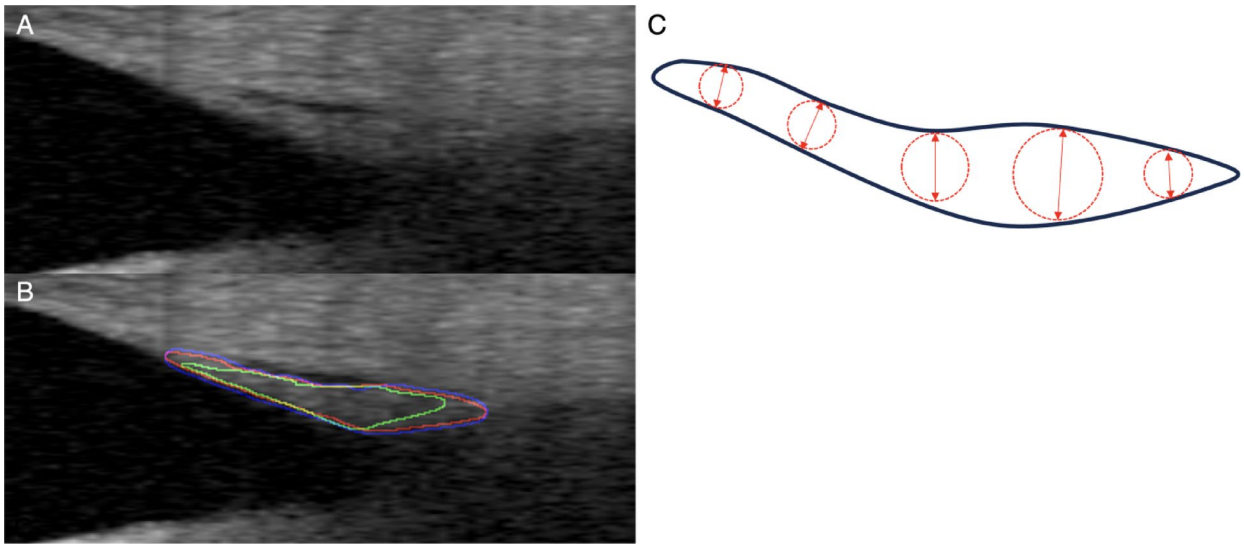

Fig. 3. Example of segmentation of trabecular meshwork (TM) in a normal eye showing the (**A**) original image, (**B**) segmentation overlain (blue – semi-automated, red – manual 1, green – manual 2) demonstrating the variability in the TM segmentation between the 2 manual segmentations as well as the semi-automated segmentation. (**C**) Diagram illustrating the ImageJ local thickness measurement as the average diameter of the largest circles (examples in red circles) that fit within the object at any point.

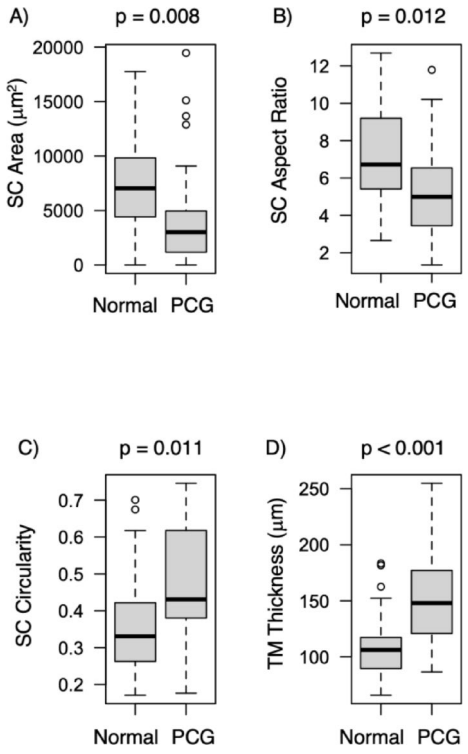

Fig. 4. Boxplot demonstrating (**A**) Schlemm canal (SC) area, (**B**) SC aspect ratio, (**C**) SC circularity, and (**D**) TM thickness for normal eyes vs. those with primary congenital glaucoma (PCG) using the semi-automated segmentation.

Discussion

We demonstrate a semi-automated segmentation algorithm that can evaluate SC and TM in children with normal eyes (controls) and those with primary congenital glaucoma. The algorithm demonstrated good performance relative to manual segmentation for evaluation of SC area. The algorithm had satisfactory performance relative to manual segmentation for evaluation of SC aspect ratio, TM thickness, and SC circularity.

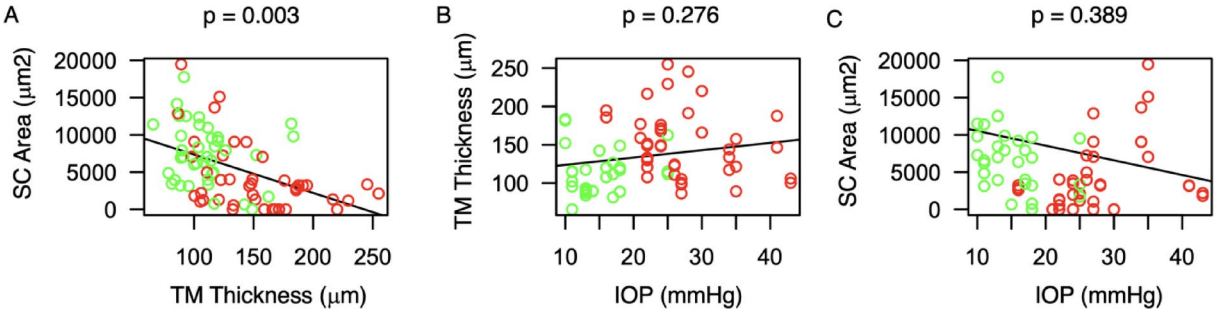

Fig. 5. Scatterplot demonstrating the association between (**A**) Schlemm canal (SC) area and trabecular meshwork (TM) thickness, (**B**) TM thickness and intraocular pressure (IOP), (**C**) SC area and IOP using the semi-automated segmentation. Green – normal, red – primary congenital glaucoma.

In our evaluation, we found that SC area was the most consistent parameter across the manual and semi-automated segmentation with high ICC. SC area is reliable because small changes in outlining the SC do not tend to dramatically alter the area, even while having a potentially larger effect on measured aspect ratio and circularity. In addition, the outline of the SC is often easier to identify as it is a small isolated hyporeflective region. In our semi-automated segmentation, we also demonstrate that the smaller SC in PCG is often more circular with lower aspect ratio. Further 3D studies beyond the scope of this pilot study are required to fully characterize SC and the TM in disease states. There was more variability in how the manual segmentation did with respect to TM thickness, which is likely secondary to the outline of the TM being harder to identify (Fig. 3).

The findings of increased TM thickness and decreased SC area in PCG are pathologic findings that have been characterized in histology[11,12] and shown in vivo. In general, there is increased TM thickness and decreased SC area in PCG compared to normal. Notably, there is significant overlap between the two groups (Fig. 4). While histopathologic studies[12] have shown a positive association between IOP and TM thickness, we did not find that association in this study.

Interestingly, there is a negative association between SC area and TM thickness even when accounting for the effect of diagnosis on the relationship. It is possible that a thicker and more anteriorly inserted TM creates less room for a patent SC regardless of whether an eye has glaucoma or not. The role this plays, if any, in IOP control and glaucoma risk requires further investigation.

Limitations

Due to the rarity of the condition and constraint on imaging time, there are number of limitations to this study. There is a limited sample size due to a small pool of young subjects undergoing clinically-indicated anesthesia. Due to the need to limit imaging time, and the technical challenges of imaging the angle in infants and small children under anesthesia, imaging was obtained only on a segment of nasal and temporal angle (about 10°) for each eye. Although features assessed in this manuscript show some differences in normal eyes and PCG eyes pre-angle surgery, there are likely other important features that are not yet identified or quantified.

As manual segmentation needed to be performed, selected representative slices were chosen from the scans and not every single scan in the volume was manually segmented. This led to an overestimation of SC area in both diagnostic categories as slices with more visible SC were selected for evaluation. This is especially true in PCG eyes, where SC is known to be more frequently collapsed.

The correlations of the structural parameters with IOP were done in setting of these eyes being on multiple glaucoma drops, which could affect the association between these structural features and IOP and may be a reason why we did not find statistically significant associations between measured structural parameters and IOP at imaging. Ethical considerations prevented us from 'washing out' glaucoma drops prior to examination in the eyes with PCG, many of which then immediately underwent planned surgery after imaging.

Manual segmentation 1 was performed by an ophthalmologist with significantly more experience with evaluating anterior segment OCT images, which may help explain the difference noted between the manual segmentations and the semi-automated segmentation. Notably, the association of smaller and more circular SC in PCG holds regardless of whether the segmentation from manual 1, manual 2, or the semi-automated measure is used.

Conclusions

We demonstrate here a semi-automated segmentation algorithm with good correlation to manual segmentation for evaluation of the SC and TM. Our results indicate that there are differences in the SC and TM morphology between normal eyes and those with PCG prior to any intraocular surgery. The semi-automated algorithm will permit 3D segmentation to be used in larger studies of how the outflow structures differ in various forms of pediatric glaucoma.

Data availability

The datasets used and/or analysed during the current study are available from the corresponding author on reasonable request.

Received: 30 October 2024; Accepted: 1 April 2025
Published online: 12 April 2025

References

1. Ko, F., Papadopoulos, M. & Khaw, P. T. Chapter 9 - Primary congenital glaucoma. in *Progress in Brain Research* (eds. Bagetta, G. & Nucci, C.) vol. 221 177–189 (Elsevier, 2015).
2. Beck, A. D. Primary congenital glaucoma in the developing world. *Ophthalmology* **118**, 229–230 (2011).
3. Barkan, O. Pathogenesis of congenital glaucoma: gonioscopic and anatomic observation of the angle of the anterior chamber in the normal eye and in congenital glaucoma. *Am. J. Ophthalmol.* **40**, 1–11 (1955).
4. Beck, A. Diagnosis and management of pediatric glaucoma. *Ophthalmol. Clin. N Am.* **14**, 501–512 (2001).
5. Shan, J., DeBoer, C. & Xu, B. Y. Anterior segment optical coherence tomography: applications for clinical care and scientific research. *Asia-Pac J. Ophthalmol. Phila. Pa.* https://doi.org/10.22608/APO.201910 (2019).
6. Hong, J. et al. Spectral-Domain optical coherence tomographic assessment of Schlemm's Canal in Chinese subjects with primary Open-angle glaucoma. *Ophthalmology* **120**, 709–715 (2013).
7. Forgačova, V. Schlemms Canal in OCT images in glaucoma patients and healthy subjects. *J. Clin. Exp. Ophthalmol.* **04**, (2013).
8. Wang, B., Naithani, R., Alvarez, S., Glaser, T. & Freedman, S. F. Vivo assessment of the pediatric trabecular meshwork, schlemm canal, and iridocorneal angle using Overhead-Mounted optical coherence tomography. *Am. J. Ophthalmol.* **269**, 402–408 (2025).
9. Abramoff, M. D., Magalhães, P. J. & Ram, S. J. Image processing with ImageJ. *Biophotonics international* (2004). http://dspace.library.uu.nl/handle/1874/204900
10. Hildebrand, T. & Rüegsegger, P. A new method for the model-independent assessment of thickness in three-dimensional images. *J. Microsc.* **185**, 67–75 (1997).
11. Anderson, D. R. The development of the trabecular meshwork and its abnormality in primary infantile glaucoma. *Trans. Am. Ophthalmol. Soc.* **79**, 458–485 (1981).
12. Agarwal, R. et al. Correlation of histopathology of trabecular meshwork with clinical features in primary congenital glaucoma. *Br. J. Ophthalmol.* **106**, 60–64 (2022).

Author contributions

B.W., A.G. and S.F. wrote the main manuscript text and prepared the figures. All authors (B.W., A.G., R.N., S.A., R.S., and S.F.) recruited patients into the study, performed imaging, and performed data entry. All authors (B.W., A.G., R.N., S.A., R.S., and S.F.) reviewed and edited the manuscript.

Funding

This study was funded by a Knights Templar Eye Foundation Career Starter Grant (147769).

Declarations

Competing interests

S.F. has an OCT device on loan from Spectralis, which was used to perform this study.

Additional information

Supplementary Information The online version contains supplementary material available at https://doi.org/10.1038/s41598-025-96963-y.

Correspondence and requests for materials should be addressed to B.W.